Fano Factor in Germanium at 77°K*

HANS R. BILGER†
Argonne National Laboratory, Argonne, Illinois

(Received 15 May 1967)

The Fano factor in germanium at liquid-nitrogen temperature has been found to be $F=0.129\pm0.003$ using γ rays at energies from 0.122 to 4.8 MeV. F appears to be independent of the primary energy in the investigated energy range. Care has been exercised to eliminate the influence of ballistic deficit, recombination, and trapping in planar lithium-drifted structures as well as noise, drift, and pile-up in the apparatus. Measurements with crystals having volumes from 0.8 to 13 cm gave consistent results. We examined the line shift and the linewidth dependence up to and into electric field strengths where saturation of electron and hole velocities occurs.

INTRODUCTION

IN an event where an ionizing particle is completely stopped in matter, the Fano factor F is defined as

$$\langle(N-\bar{N})^2\rangle=F\bar{N}, \tag{1}$$

where N, $(\bar{N})$ is the (average) number of produced pairs;

$$\bar{N}=E/\epsilon, \tag{2}$$

where E is the initial energy of the ionizing particle (eV) and ϵ is the average energy expended per pair (eV/pair). The resulting spectroscopic root-mean-square (rms) linewidth σ is then given as

$$\sigma(\text{eV})=\epsilon[\langle(N-\bar{N})^2\rangle]^{1/2}=(\epsilon FE)^{1/2}, \tag{3a}$$

or, if the distribution is Gaussian,

$$\Delta E_{\text{FWHM}}=[8(\ln 2)\epsilon FE]^{1/2}, \tag{3b}$$

where ΔE_{FWHM} is the full width at half-maximum (eV). From values given in the literature[1–4] we have adopted[1] $\epsilon=2.98\pm0.01$ eV/pair for γ rays throughout this paper. F has only recently received attention.[5–7] Experimental estimates of F in germanium range from 0.155 [8] to 0.30 [1] to 0.4 [9] to higher values.[7] In this paper, investigations are described with the exclusive goal of determining the best value of the intrinsic Fano factor[10] by eliminating, reducing, or evaluating the sources of systematic errors, which in general tend to increase the observed F.

After a brief discussion of the theoretical situation on F, the sources of systematic errors are described and the method of measurement is given. Then the measurements at specific γ energies are presented. Finally, an appraisal of the significance of the results is given.

THEORETICAL SITUATION

The ionization processes have been described in the literature.[6,7,11] F is defined as the variance of the number of pairs in the process of creation only. Therefore, it is necessary to separate out losses (or secondary creation) and fluctuations of these losses during the collection process. This is facilitated by the fact that the losses in good detectors are typically of the order of 10^{-3} (see Table III).

Since the creation of the pairs is a multistage process, it is not unreasonable to assume a Poisson distribution of N, which results in $F=1$. However, applying Fano's ideas[12] to semiconductors[6] one can anticipate $F=0.1$ to 0.2.[13] In an entirely different approach, W. van Roosbroeck[5] uses a statistical model ("crazy carpentry") to calculate F and ϵ as a function of phonon losses. In the semiconductor case $F=1$ and $F\simeq0.12$ are the limiting values for large and for no-phonon losses, respectively.

Numerical estimates of F and ϵ can easily be obtained through Fano's calculations under simplified conditions (see Fig. 1). Under the assumption that phonon production makes a negligible contribution to F, and all transition cross-sections σ_{ij} are equal, we have[12]

$$F=[(m+1)(n+1)]^{-1}\sum_{i=0}^{m}\sum_{j=0}^{n}(1-E_{ij}/\epsilon)^2, \tag{4}$$

and

$$\epsilon=[(m+1)(n+1)]^{-1}\sum_{i=0}^{m}\sum_{j=0}^{n}E_{ij}. \tag{5}$$

* Work produced under the auspices of the U.S. Atomic Energy Commission.

† On leave of absence from Oklahoma State University, Stillwater, Oklahoma.

[1] S. O. W. Antman, D. A. Landis, and R. H. Pehl, Nucl. Instr. Methods **40**, 272 (1966).

[2] W. Shockley, Czech. J. Phys. **B11**, 81 (1961).

[3] J. Tauc, Rev. Mod. Phys. **29**, 308 (1957).

[4] F. E. Emery and T. A. Rabson, Phys. Rev. **140**, A2089 (1965).

[5] W. van Roosbroeck, Phys. Rev. **139**, A1702 (1965).

[6] G. D. Alkhazov, A. A. Vorob'ev and A. P. Komar, Bull. Acad. Sci. USSR Phys. Ser. **29**, 1231 (1965); G. D. Alkhazov, A. P. Komar and A. A. Vorob'ev, Nucl. Instr. Methods **48**, 1 (1967).

[7] A discussion of literature about F up to 1965 is given in G. Dearnaley and D. C. Northrop, *Semiconductor Counters for Nuclear Radiation* (E. and F. N. Spon Ltd, London, 1966), 2nd ed.

[8] R. L. Heath, W. W. Black, and J. E. Cline, IEEE Trans. Nucl. Sci. **NS-13**, 445 (1966).

[9] G. T. Ewan, Bull. Acad. Sci. USSR, Phys. Ser. **29**, 1057 (1965).

[10] H. R. Bilger and H. M. Mann, Bull. Am. Phys. Soc. **11**, 127 (1966).

[11] H. R. Bilger and H. M. Mann, in Symposium on Fluctuation Phenomena, Minneapolis, 1966 (unpublished).

[12] U. Fano, Phys. Rev. **72**, 26 (1947).

[13] O. Meyer and H. J. Langmann, Nucl. Instr. Methods **39**, 119 (1966).

(See Fig. 1 for an explanation of the symbols.) These sums are evaluated using equidistant levels in the bands. In the limit $m\to\infty$, $n\to\infty$, one obtains

$$F=\tfrac{1}{3}(\alpha^2+\beta^2)/(\alpha+\beta+2)^2, \quad (6)$$

and

$$\epsilon=\Delta E+\tfrac{1}{2}\alpha\Delta E+\tfrac{1}{2}\beta\Delta E, \quad (7)$$

where ΔE is the band gap, $\alpha\Delta E$ is the width of the conduction band, and $\beta\Delta E$ is the width of the valence band. Equation (7) provides the obvious result that the average transition takes place from band center to band center. From Eq. (6), we find that F is symmetric in the bands and not dependent on ΔE. Furthermore, $0\leq F\leq\frac{1}{3}$. The lower limit is obtained if both bands have vanishing widths (transition between two levels, $\alpha=\beta=0$); the upper limit, if one of the bands is very large.

WHY USE γ RAYS?

In this investigation γ rays are used exclusively, for the following reasons:

1. There are no window problems, either in the source or in the detector. Since γ rays produce ionizing particles after entering the solid, there are no penetration losses through the boundary of the crystal (detector), as there are with electrons. Heavier particles like p, α, He^+, etc., have the added disadvantage of producing additional fluctuations through nuclear collisions.[14,15] We do not include these fluctuations in the definition of F.

2. Since practically the only reaction products of γ rays are electrons and positrons (plus additional photons) with relatively small energy loss per length (dE/dx), the ionization density is small and the collection of the final electron-hole pairs is facilitated.

3. A monoenergetic photon with $E>2m_0c^2$ (m_0c^2= rest energy of an electron) produces 3 lines with a separation corresponding to the well-known energy m_0c^2. This may serve to establish an energy scale without the need of using $E=0$ as a reference.

4. Many γ sources can be obtained with closely spaced well-known energies from the x-ray region up to several MeV, with reasonable intensities and half-lives.

5. The obvious need for large-volume detectors[16] has the advantage of resulting in a device with a uniform electric field, which can be adjusted over a certain range, if planar detectors are used.[17]

In the following, some processes are discussed which affect the linewidth but are unrelated to F (line-broadening effects).

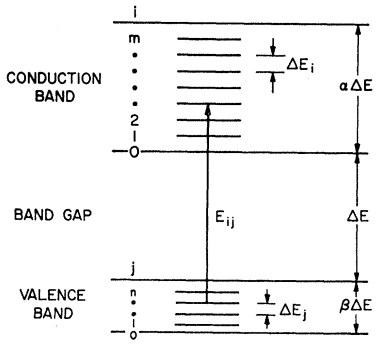

FIG. 1. Model of a transition scheme with a bandgap ΔE, a valence band of width $\beta\Delta E$, and a conduction band $\alpha\Delta E$. The bands are composed of m and n equidistant energy levels, respectively, $(m\to\infty, n\to\infty)$, with an energy-independent transition cross section. No phonon losses are assumed. The model results in $0\leq F\leq\frac{1}{3}$.

[14] P. Siffert, A. Coche, and F. Hibou, IEEE Trans. Nucl. Sci. **NS-13,** 225 (1966).

[15] J. Lindhard, V. Nielsen, M. Scharff, and P. V. Thomsen Kgl. Danske Videnskab. Selskab., Mat.-Fys. Medd. **33,** No. 10 (1963).

SOME DETAILS ON THE COLLECTION OF CREATED PAIRS

The collection process takes a time of the order of 10^{-7} sec in thick detectors (more than 1-cm thickness).[18] During this process, carriers can be lost, which may add to the observed fluctuation of N and increase the apparent Fano factor.[19] Therefore, we varied the electric field strength in all measurements.

Recombination and Trapping

A simple approach[20] yields

$$\langle\Delta N_{\rm rec}\rangle=\bar{N}_0 d/\mu\tau e=\alpha/e, \quad (8)$$

where $\langle\Delta N_{\rm rec}\rangle$ is the average number of recombining (trapped) pairs, or

$$\langle\Delta E_{\rm rec}\rangle=\langle\Delta N_{\rm rec}\rangle\times\epsilon=E\times d/\mu\tau e, \quad (9)$$

where $\bar{N}_0$ is the initial number of created pairs, d is the thickness of detector (m), e is the electric field strength (V/m), μ is the mobility (m^2/Vsec), τ is the lifetime of carriers (sec), $\langle\Delta E_{\rm rec}\rangle$ is the energy equivalent of the number of recombining pairs[21] (eV), and

$$\langle(\Delta N_{\rm rec}-\langle\Delta N_{\rm rec}\rangle)^2\rangle=\sigma^2=\langle\Delta N_{\rm rec}\rangle=\alpha/e, \quad (10a)$$

[16] According to tables obtained by interpolation of γ-ray attenuation coefficients from neighboring elements [W. Snow, Argonne National Laboratory report, 1967 (unpublished)], the minimum mean length before interaction of γ rays in germanium (at about 8 MeV) is 6.1 cm.

[17] H. M. Mann, F. J. Janarek, and H. W. Helenberg, IEEE Trans. Nucl. Sci. **NS-13,** 336 (1966).

[18] M. G. Strauss, R. N. Larsen, and L. L. Sifter, IEEE Trans. Nucl. Sci. **NS-13,** 265. (1966)

[19] On the other hand, there is the possibility that in some cases small apparent Fano factors are obtained due to multiplication of carriers in zones with high electric fields. Such an effect can be excluded in our measurements (see section on measurements and results), because the observed pulse heights typically vary by less than 1% over a wide range of applied voltage. Besides, multiplication processes are statistical and therefore themselves introduce additional fluctuations [R. H. Haitz and F. M. Smits, IEEE Trans. Nucl. Sci. **NS-13,** 198 (1966)].

[20] H. M. Mann, H. R. Bilger, and I. S. Sherman, IEEE Trans. Nucl. Sci. **NS-13,** 252 (1966).

[21] Since ϵ is considered to represent strictly the ratio (γ energy)/(number of created pairs) in the first stage of events (see introduction), ϵ is necessarily independent of the details of the collection process.

or

$$\sigma^2(\mathrm{eV}^2)=\epsilon^2\langle\Delta N_{\mathrm{rec}}\rangle=\alpha/e. \qquad (10b)$$

More sophisticated information can be found elsewhere.[7,22] Equations 10 are obtained by assuming the recombination to be a purely random process with Poisson statistics.

A plot of $\langle\Delta E_{\mathrm{rec}}\rangle$ as well as of σ^2 versus $1/e$ can be used to extrapolate $\bar{N}$ and σ^2 to infinite field strength in order to obtain the intrinsic Fano factor.

In cases of low field strength and/or nonuniform residual impurity content in a detector, the loss process of carriers may be quite different from Poissonian, as is demonstrated by "tails" on the distribution of N (the lines).

Ballistic Deficit

It has been found[18] that in lithium-drifted detectors of thickness larger than a few millimeters, the current pulses due to incident γ rays have large fluctuations in time. The fluctuations are due to the different spatial distribution of the created carriers for different photons. The rise-time fluctuations are of the same order of magnitude as the pulse duration itself, which is 10^{-7} sec. Since the measurement of the total charge output is done ballistically,[23] there appears a slight pulse-height defect for any current pulse of finite duration. If we have a rectangular current pulse of duration T and a simple RC–RC-shaped output pulse with $RC=\tau$, then the deficit, expressed as the fraction of lost pairs $\Delta N/N_0$, is

$$\Delta N/N_0=\beta(T/\tau)^2, \qquad (11)$$

with $\beta=\frac{1}{24}$.

As an example, if $T=2\times10^{-7}$ sec and $\tau=2\times10^{-6}$ sec, then $\Delta N/N_0=4.2\times10^{-4}$, which is equal to the relative linewidth σ/E of detectors at 2.2 MeV. For different current pulse shapes, the coefficient β in Eq. (11) will vary, but in a first-order approximation the quadratic dependence of T/τ will be preserved[24] (see Appendix). So the use of several time constants for the filter will be important in the diagnosis of the influence of any fluctuation of the current pulse durations on the line shape.

PROBLEMS ASSOCIATED WITH THE MEASUREMENT OF THE CHARGE DISTRIBUTION

Noise

Since N is obtained by measuring the resulting charge at the electrodes of the detector, the electronic noise charge detector circuit (a charge-sensitive preamplifier[25]) will produce additional fluctuations; so will the leakage current of the detector.[7,26] This type of fluctuation can be reduced by careful preparation of the detector,[17] by proper choice of the amplifying elements at the input and in the circuitry, and by careful input layout.[27] In practice, noise will be the most important source of fluctuation besides F.

Pileup

Usually the time constants of the amplifiers are given by considerations regarding noise and ballistic deficit. Pole-zero cancellation is applied in the high-energy measurements to ensure fast base-line recovery (see section on apparatus). Thus, the only remaining thing to do is to reduce the count rate in a given experiment until the linewidths are no longer sensitive to the count rate.

Drift of Gain or Threshold

Special high-feedback electronics is used to reduce the drift during a run. The requirements are illustrated by the fact that relative linewidths of less than 10^{-3} have to be measured with an accuracy of better than 10%, which requires drifts of less than 100 ppm of the total apparatus during a run.

APPARATUS

A block diagram is given in Fig. 2.

Detector and Preamplifier

The detector and a first stage including a field-effect transistor are mounted close together on a liquid-nitrogen-cooled cold finger inside a vacuum system. The input capacitance of the first stage excluding the detector is about 8 pF. The preamplifier[28] provides a charge-sensitive loop with an open-loop gain $>10^5$. The noise of these systems (excluding the detector) ranges from 58 rms pairs charge equivalent (410-eV FWHM equivalent energy spread) on up, depending on the quality of the first transistor and the input circuitry. Li-drifted planar detectors with volumes between 0.8 and 13 cm^3 were used in the measurements.

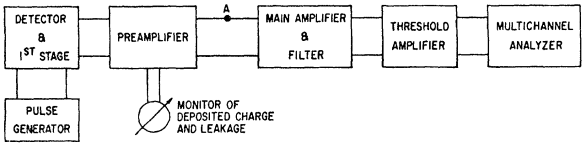

FIG. 2. Block diagram of the apparatus to measure F. The pulse from the pulse generator is injected into the input through a capacitor of 0.5 pF, approximately. Some description of the units is given in the text.

[22] R. B. Day, G. Dearnaley, and T. M. Palms, IEEE Trans. Nucl. Sci., **NS-14**, 487 (1967).

[23] E. Baldinger and W. Franzen, Advances Electron. and Electron Phys. **VIII**, 255 (1956).

[24] The help of R. G. Roddick, Argonne National Laboratory, in these matters is gratefully acknowledged.

[25] E. Fairstein and J. Hahn, Nucleonics **23**, 56 (1965); *ibid.* **24**, 68 (1966).

[26] L. Scott and M. J. O. Strutt, Solid-State Electron. **9**, 1067 (1966).

[27] Hans R. Bilger, Nucl. Instr. Methods **40**, 54 (1966).

[28] The preamplifier after the input stage was designed by I. S. Sherman, Argonne National Laboratory.

TABLE I. Information about the γ sources.

Sources	Half-life	Investigated energies E_γ (MeV)	Energy difference between lines $\Delta E\gamma$ (KeV)
^{57}Co	268 day	0.12197–0.13633	14.36[a]
^{133}Ba	7.2 yr	0.35625–0.38409	27.83[b]
^{60}Co	5.26 yr	1.173226–1.332483	159.257[a]
^{208}Tl(ThC″)–^{24}Na	$(1.4\times10^{10}$ yr)–15.0 h	2.61447–2.75392	139.45[a]
^{208}Tl(ThC″)	$(1.4\times10^{10}$ yr)	2.61447–(2.61447–m_0c^2)	511.006[a]
^{66}Ga	9.5 h	(4.2950–$2m_0c^2$) (4.4616–$2m_0c^2$) (4.8059–$2m_0c^2$)	166.6–344.3[c,d]
^{66}Ga	9.5 h	(4.8059–$2m_0c^2$)–4.2950	511.1[c]
^{66}Ga	9.5 h	4.2950–4.8059	510.9[c]

[a] J. B. Marion, California Institute of Technology (private communication).
[b] J. E. Thun, S Törnkvist, K. Bonde Nielsen, H. Snellman, F. Falk, and A. Mocoroa, Nucl. Phys. **88**, 289 (1966).
[c] Reference 38.
[d] The help of M. C. Oselka, who was responsible for the deuteron irradiation of M. S. Freedman in preparing and handling the source is gratefully acknowledged.

Main Amplifier

A Tennelec TC 200 was used at the lower energies, and a pole-zero-cancelled design[29] at high energies. An added feature of the latter amplifier was a built-in bias restorer which insures quick baseline recovery through the use of nonlinear circuitry (diodes).

Threshold Amplifier

This device[30] was used to cut off pulse heights at a predetermined level. The introduction of a threshold was necessary in order to reduce the channel requirements of the following multichannel analyzer and to reduce pileup problems at the following stages. This design also has the advantage of delivering a normalized output pulse shape especially suited for analyzer inputs.

Pulse-Height Analyzer

In the following measurements, three different analyzers were employed with success: a 400 channel RIDL, an 800 channel Victoreen, and a 1600 channel Victoreen Scipp analyzer. No servo-stabilized systems were used for the measurements reported in this paper.

Pulse Generator

A Berkeley Nucleonics Corporation stable pulser with a specified drift of 0.003%/°C (30 ppm/°C) was used.

SOME TESTS OF THE APPARATUS

Any fluctuation of the pulser amplitude (or a fluctuation of the capacitor which injects the charge into the first stage) would simulate excessive noise of the system and consequently result in a low apparent F (through quadratic subtraction of the noise; see evaluation of the data). On the other hand, a line-synchronized pulser rate tends to increase F if there is residual hum at the output.

The repetition rate was usually between 0.1 and 10 pulses/sec (not synchronized with the line frequency). The results of short runs indicated that the stability was sufficient. To check on short-term fluctuations of the pulser, the pulse was introduced at point A (see Fig. 2) with the preamplifier switched off. The main amplifier was then adjusted to produce a line at the same channels on the analyzer. The width of the line was in all cases about an order of magnitude smaller than after insertion of the pulse at the front end.

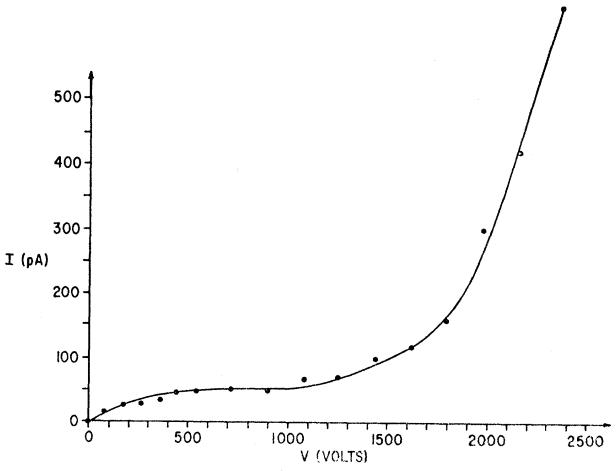

FIG. 3. Example of a I-V characteristic achieved with a 3.5-cm³ detector (Geli 52). Spectra were taken with voltages up to 1800 V.

[29] This design was made by M. G. Strauss *et al.*, Argonne National Laboratory.
[30] Designed by R. G. Roddick, Argonne National Laboratory.

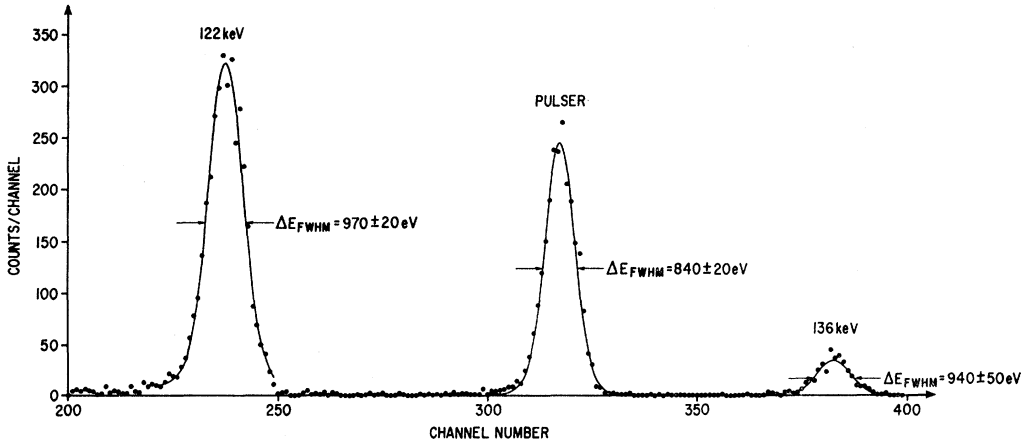

FIG. 4. Spectrum obtained from a ^{57}Co source with Geli 52. The energy spread is 99.1 eV/channel. The solid lines are least-squares-fitted Gaussians. The errors of the full widths at half-maximum (FWHM) are calculated from the standard deviations as supplied by the computer program.

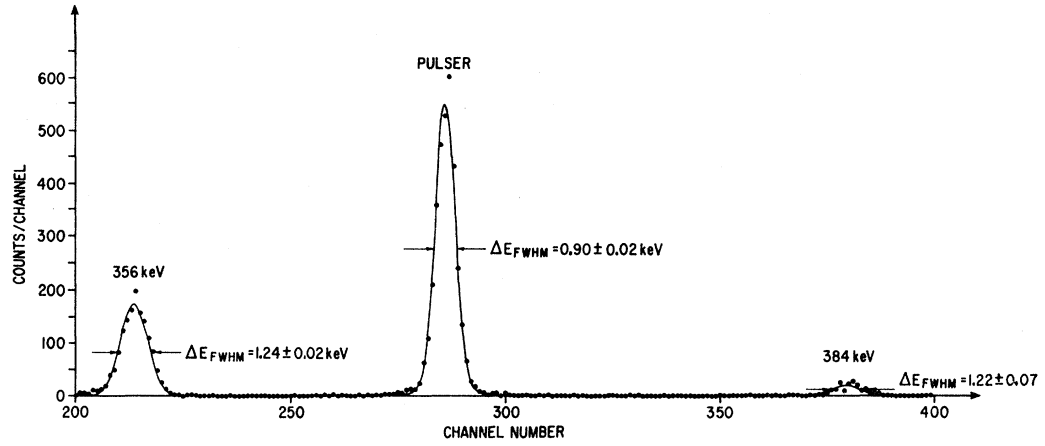

FIG. 5. Spectrum obtained from a ^{133}Ba source with Geli 52. The 0.384-keV line merely serves to define the energy scale.

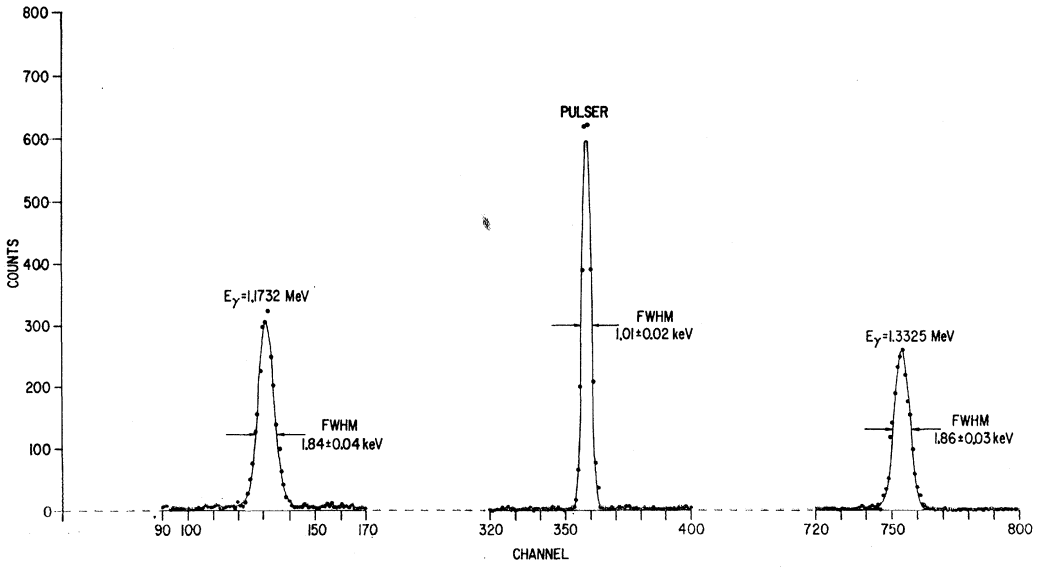

FIG. 6. Spectrum obtained from a ^{60}Co source with Geli 52. Channels 170 to 320 and 400 to 720 have been eliminated in order to spread the lines. RMS errors are given.

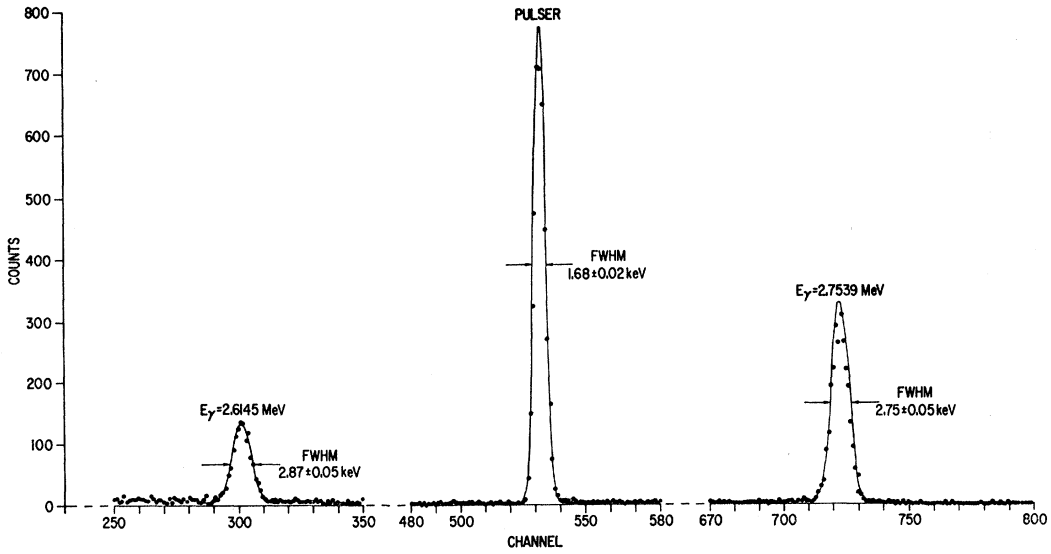

FIG. 7. Spectrum obtained from a ^{208}Tl(ThC'') and a ^{24}Na source with Geli 52. Channels 350 to 480 and 580 to 670 have been eliminated. The pulser line shows broadening in this experiment. RMS deviations are given.

PERFORMANCE OF THE EXPERIMENTS

Sources

The investigations centered around the sources which are given in Table I. (The immediate parents are given, as is customary.) The errors in the energy differences are small enough to be neglected in the error analyses.

An attempt to measure F with neutron-capture γ rays from ^{64}Cu ($Q=7.91$ MeV [31]) was unsuccessful. The failure is attributed to pileup. (At the time of the measurement, pole-zero cancellation had not yet been introduced.)

At least two γ lines were recorded in each measurement with a pulse line generated between the lines. The sources were chosen according to the criteria given above. The rate was monitored by measuring the change of the dc current through the detector, which could be done by simply watching the feedback voltage at the bottom of the detector load resistor.[28,32] The pulser line is used to measure the noise of the system, includ-

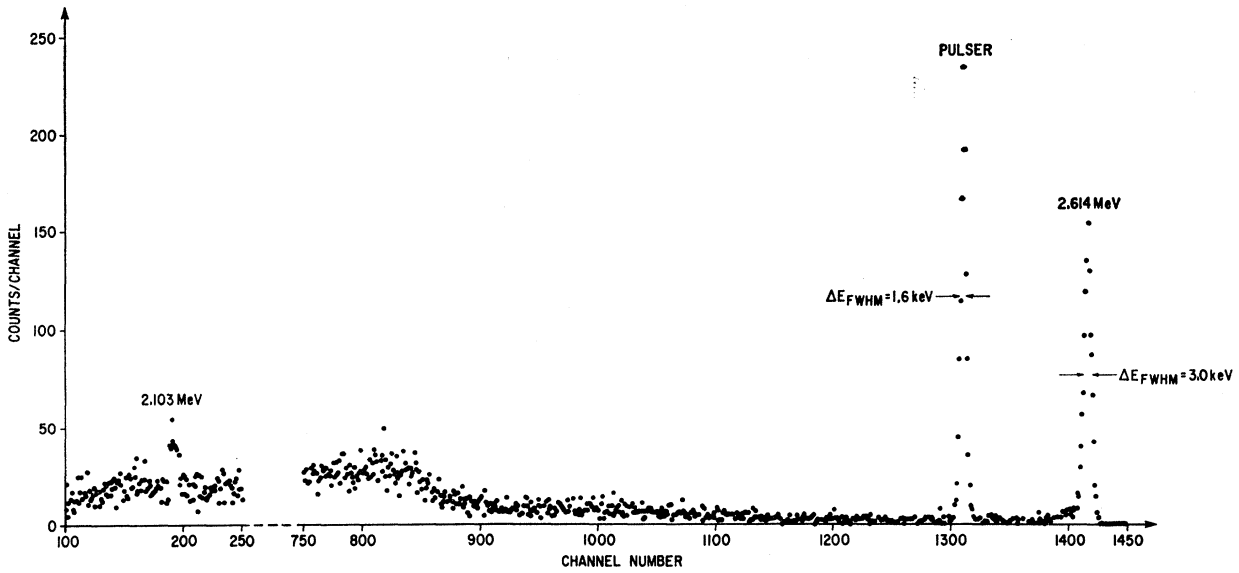

FIG. 8. Spectrum containing the full-energy line, the pulser line, and the single-escape line from ^{208}Tl(ThC''). Channels 250 to 750 are omitted. The full-energy peak-to-Compton ratio is about 6:1. Geli 123 with 16.5 mm thickness and 13 cm^3 volume is used.

[31] We thank H. H. Bolotin, Argonne National Laboratory, for assistance in preparing this experiment at the reactor.

[32] Actually, the change of the feedback voltage is proportional to the average charge per second deposited in the detector. We consider this as a proper quantity to use to monitor the pileup.

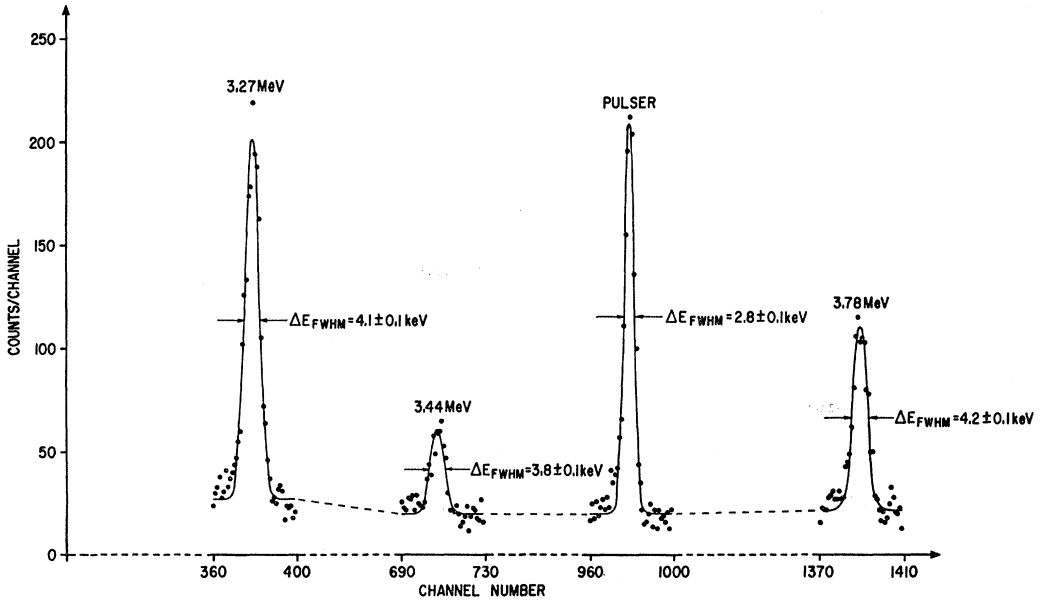

FIG. 9. Lower-energy section of the ^{66}Ga spectrum obtained through Geli 123. The measurements are done after the count rate has been reduced till the pulser linewidth was no longer count-rate-sensitive. The line at 3.78 MeV contains a doublet, which gives rise to a slight broadening in the runs. 30 min were used per run. Note that channels 400–690, 730–960, and 1000–1370 are eliminated.

ing detector noise. If the system is linear, the linewidth should be independent of the pulse height and it should indicate the basic noise in the system, predominantly that due to the detector leakage current and that in the first stage. In practice, the pulser linewidth tends to grow larger with larger pulse heights (larger energies) unless serious precautions are taken. So the pulser line, which was always run simultaneously with a given set of γ-ray energies, served as an indicator of unwanted effects in the setup. It may be noted here that the apparent F grew larger as soon as the pulser linewidths grew larger. This is so because line-broadening effects which affect both pulser and γ line usually give a positive contribution to the net linewidth or F (see Appen-

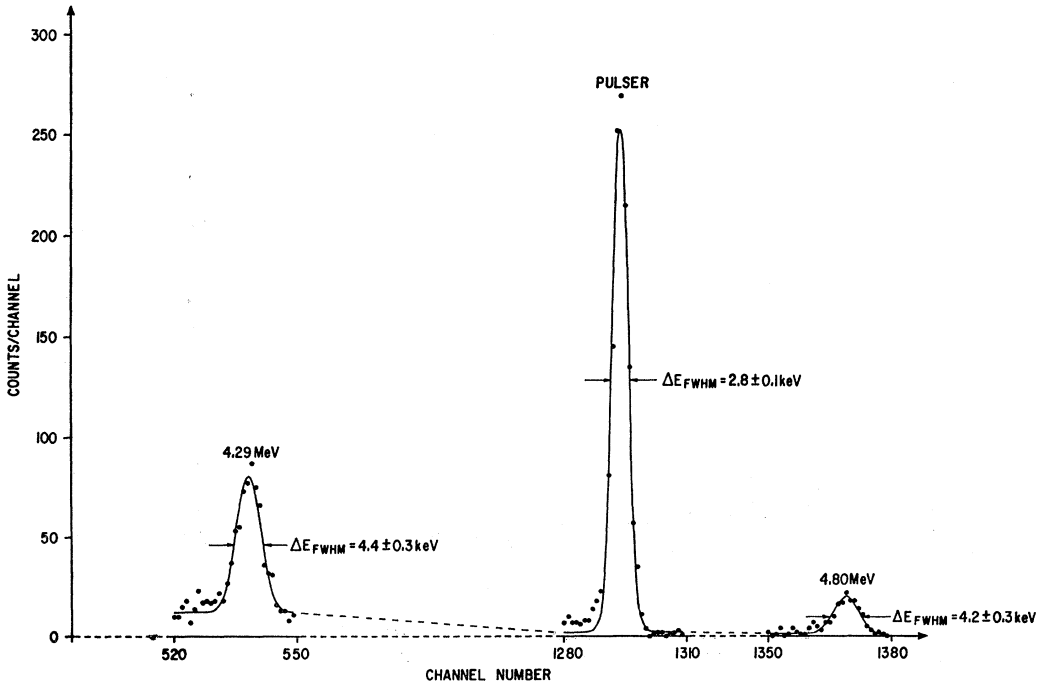

FIG. 10. Higher-energy section of the ^{66}Ga spectrum obtained through Geli 123. (See Fig. 9.) The 4.29-MeV line contains a doublet. Channels 550 to 1280 and 1310 to 1350 have been eliminated.

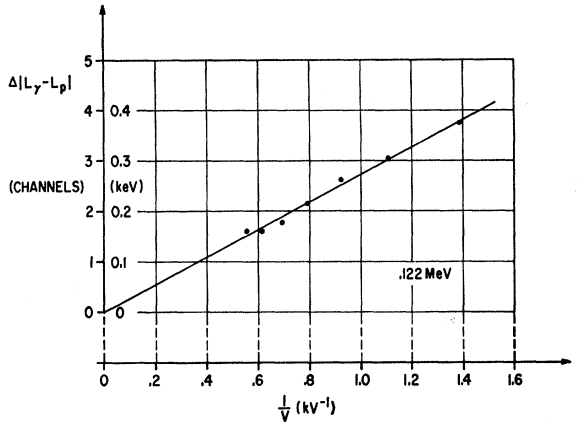

FIG. 11. Line shift of the 0.122-MeV line versus the reciprocal detector voltage. Each of the seven points is an average of four 1-min runs. The pulser location is the reference. In order to represent the field-dependent losses, the origin of the vertical scale is chosen at the intercept of the straight line representing the losses. This point corresponds to $V \rightarrow \infty$.

dix). A series of final measurements was taken only after the pulser did not deviate excessively from the linewidth at small pulse heights in a given detector system.

Linearity

Since closely spaced γ lines were used with a pulser line in between, the linearity requirements are not very stringent. However, at least one of the following three checks were made in a given experiment:

1. The pulser amplitude was adjusted to equidistant steps (of arbitrary amount) in the range of interest. The channel differences between the locations were evaluated (see next section), and if they were not constant, then corrections to the linewidths were applied (a few percent at most). The widths of the pulser lines served as an additional test of local fluctuations

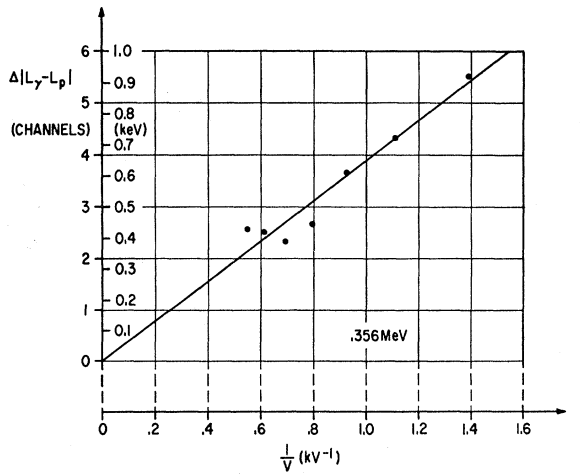

FIG. 12. Line shift of the 0.356-MeV line versus the reciprocal detector voltage. Each of the seven points is an average of four 5-min runs. The pulser location is the reference. As in Fig 11, the field-dependent losses are given on the vertical axis. The energy spread is 166.8 eV/channel.

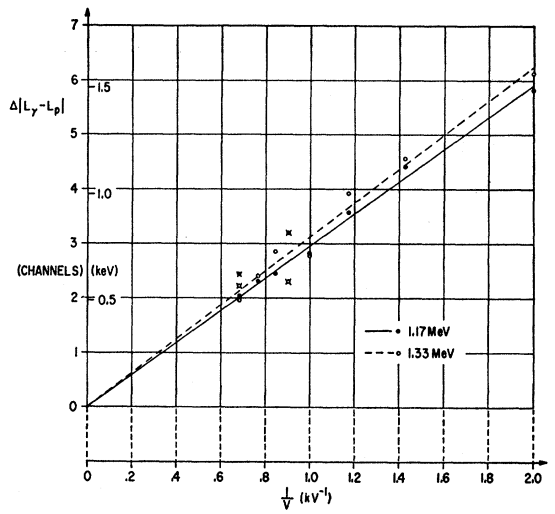

FIG. 13. Line shift of the two ^{60}Co lines versus the reciprocal detector voltage. Each point represents a 20-min run. The points with a superimposed cross were taken at the end of a regular sequence of runs and are disregarded in calculating the position of the straight line. The energy spread is 255.8 eV/channel.

of the channel widths. In all cases, we found that the pulser widths were uniform over the range of interest.

2. The threshold of the threshold amplifier was slightly changed above and below the original level. Each line appears then as a triplet and the location differences provide direct information on the differential linearity at the channels we are interested in, namely, at the γ and pulser locations.

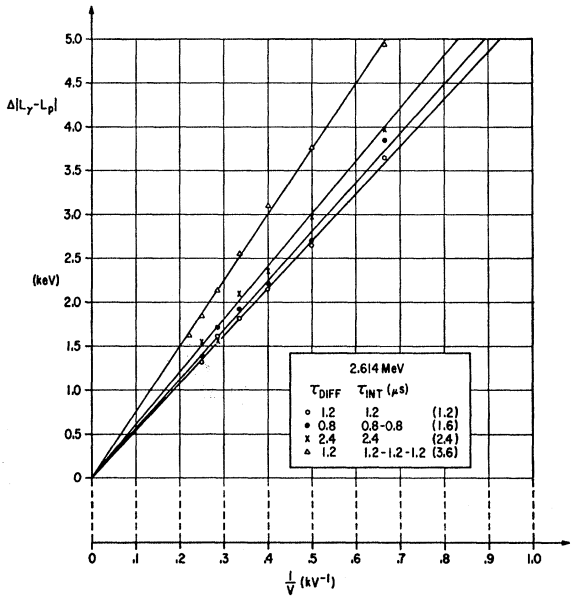

FIG. 14. Line shift of the full energy line of ^{208}Tl versus the reciprocal detector voltage. The detector thickness is 16.5 mm. Four different filter time constants have been used from 1.2 to 3.6 μsec. The dots are obtained with double integration (0.8−0.8 μsec) and the triangles with triple integration (1.2–1.2–1.2 μsec). The voltage was varied between 1.5 and 4.5 kV. The energy spread is between 427.2 and 418.0 eV/channel.

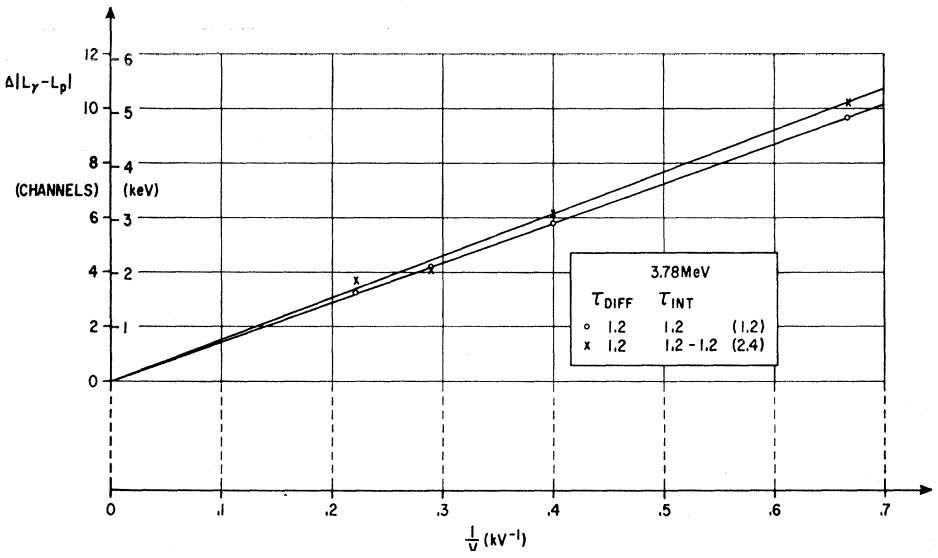

FIG. 15. Line shift of the 3.78-MeV line versus the reciprocal detector voltage for two filter time constants. The energy spread is 509 eV/channel.

3. In the ^{66}Ga measurements, a few weak lines with known energies appeared besides the investigated lines, which served as a check on the linearity.

EVALUATION OF THE DATA

Lines with Gaussian Shape

Basic noise phenomena like shot noise or thermal noise are known to be Gaussian processes.[33] Therefore, it is to be expected and in general confirmed that pulse-height fluctuations due to noise have a Gaussian distribution. The fact that the ionization processes involve a variety of mechanisms leads us to believe that the line shapes due to F are Gaussian, too. Rather than prove this belief in general, we used its validity as a criterion to accept or reject measurements.

A convolution of n Gaussian distributions results again in a Gaussian with the same center location, but with a total linewidth σ_T:

$$\sigma_T^2 = \sum_{i=1}^{n} \sigma_i^2, \tag{12}$$

where σ_i is the rms width of an individual Gaussian.

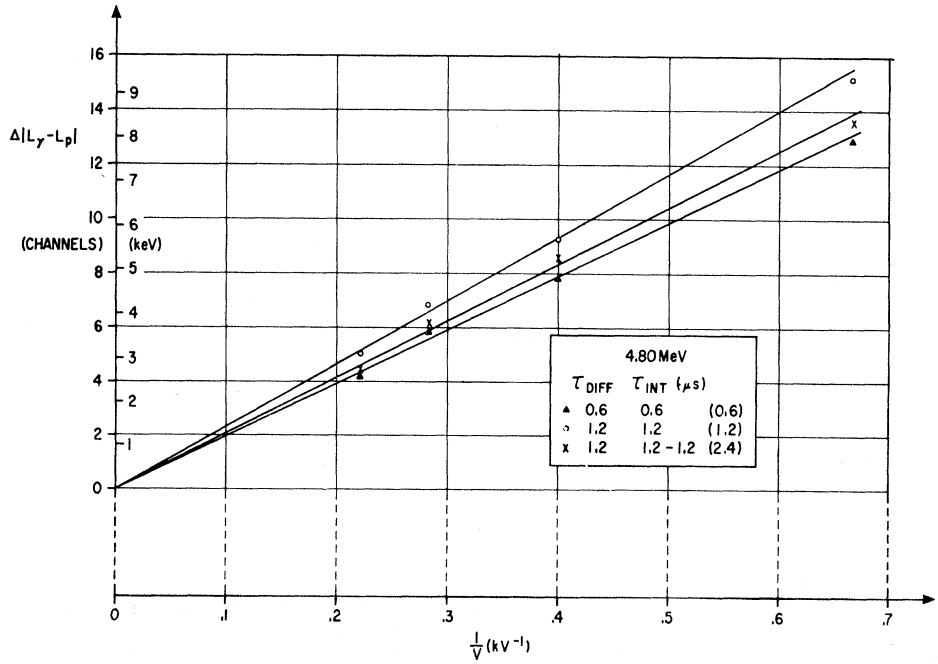

FIG. 16. Line shift of the 4.80-MeV line versus the reciprocal detector voltage. The three time constants 0.6, 1.2, and 2.4 μsec have been used; the latter was achieved by double integration. The energy spread here is 616 eV/channel.

[33] *Fluctuation Phenomena in Solids*, edited by R. E. Burgess (Academic Press Inc., New York, 1965).

TABLE II. Some results from the spectra.

Energy (MeV)	$(\sigma_\gamma-\sigma_p)/\sigma_\gamma$ typical	rms deviation of data from straight-line relation $\Delta(L_\gamma-L_p)$ versus $1/V$ (eV)	(pairs)	ΔN at V_{max} (pairs)	V_{max} (kV)	*Schubweg* at V_{max} (m)
0.122	0.1	7.5	2.5	53	1.8	10
0.356	0.4	44	15	145	1.8	12
1.17	0.5	27	9	174	1.46	32
1.33	0.5	50	17	184	1.46	34
2.61	0.4	62	21	510	4.0	28
3.78	0.3	≃100	33	580	4.5	36
4.8	0.3	≃150	50	940	4.5	28

This statement is also approximately true for distributions not much different from Gaussians.

On the basis of Eq. (12), the net width of a γ line due to F is then obtained by quadratic subtraction of the pulser width σ_p from the total width σ_γ of the γ line, after fluctuations due to collection inefficiencies are eliminated. F is then obtained through Eq. (3a).

Computer Program

A Gaussian with a constant background was fitted to each observed line:

$$y(x)=H\exp[-(x-L)^2/2\sigma^2]+B, \qquad (13)$$

where $y(x)$ is the number of counts in channel x of the analyzer, H is the number of counts in the center of the Gaussian, L is the location of the center (may be a fractional channel), σ is the rms width (channels), and B is the number of background counts. The 3600 computer program[34] employed requires an estimate H_0, L_0, σ_0, and B_0, and evaluates the best-fitted parameters H, L, σ, and B in an iteration process which minimizes

$$\chi^2=\sum_{j=1}^{n}(o_j-e_j)^2/o_j. \qquad (14)$$

Here o_j is the observed counts in channel j, e_j is the calculated counts in channel j, and n channels total (if $o_j=0\rightarrow\chi^2=1$). As a result, the computer gives the best-fitted parameters together with their standard errors (the square roots of the diagonal elements of the given error matrix).

The problem has $n-5$ degrees of freedom so that if $n-5\gg1$, the minimum χ^2 should be of this magnitude on the average.

If the $y(x)$ are Gaussian-distributed, the standard errors of the most interesting parameters L and σ are given by[35]

$$\Delta L=\sigma/N^{1/2}, \qquad \Delta\sigma=\sigma/(2N)^{1/2}, \qquad (15)$$

where N is the total number of counts in the distribu-

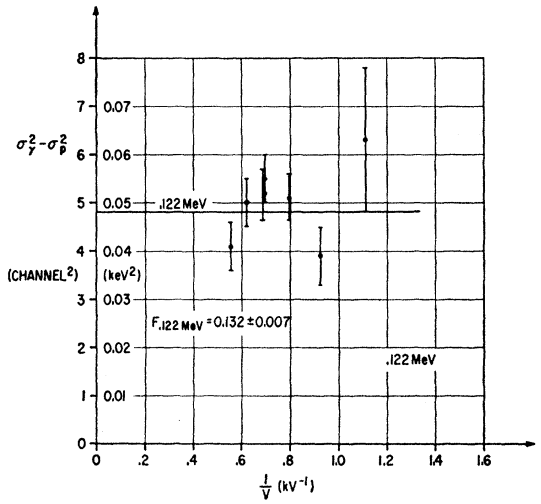

FIG. 17. Net squared rms linewidth $(\sigma_\gamma^2-\sigma_p^2)$ versus the reciprocal detector voltage. The detector thickness is 14 mm. Each point is an average of four 1-min runs. The error of F is the rms deviation of the average of the six runs above 1 kV.

[34] Thanks are due to J. D. Simpson, Argonne National Laboratory for making the program available and to J. P. Marion for modifications.

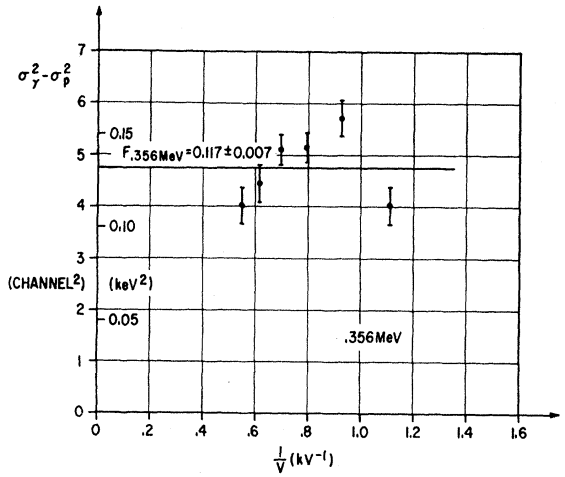

FIG. 18. Net squared rms linewidth $(\sigma_\gamma^2-\sigma_p^2)$ versus the reciprocal detector voltage (14 mm thickness). Each point is an average of four 5-min runs. The error of F is the rms deviation of the six runs presented.

[35] J. Orear, University of California Radiation Laboratory Report No. UCRL-8417, 1958 (unpublished).

TABLE III. Evaluation of the line shifts.

Energy (MeV)	$\Delta(L_\gamma - L_p)/\Delta(1/v)$ (channels×kV)	$(\Delta N_{rec}/N_0)$ $e=1$ kV/cm	$\mu\tau_{eff}$ (cm²/V)	Detector thickness (mm)
0.122	0.270	1.58×10^{-3}	0.9	14
0.356	0.648	1.30×10^{-3}	1.1	14
1.17	0.758	0.46×10^{-3}	3.0	14
1.33	0.798	0.43×10^{-3}	3.3	14
2.61	6.1	1.42×10^{-3}	1.2	16.5
3.78	7.6	1.22×10^{-3}	1.4	16.5
4.80	13.1	1.65×10^{-3}	1.0	16.5

tion. The observed N will be closely approximated by

$$N_{calc}=\int_{-\infty}^{+\infty} H\exp[-(x-L)^2/2\sigma^2]dx=(2\pi)^{1/2}H\sigma. \tag{16}$$

Thus, if $N=10^3$, then $\Delta L/\sigma\approx3\%$ and $\Delta\sigma/\sigma\approx2\%$ are to be expected. In some cases, runs were made with N as low as 100.

It should be pointed out that χ^2_{min} was usually somewhat higher than $n-5$. This can be attributed to the fact that o_j becomes quite small in the tails of the distribution, and the contribution to χ^2 from the tails may reach a sizable fraction. No measures were taken to alleviate this problem, apart from experimental precautions of avoiding drift, pileup, etc.

MEASUREMENTS AND RESULTS

The accessible energy range is limited at the lower end by the noise of the system (in our case the smallest noise with germanium detector was about 0.8 keV FWHM [36]), whereas at the upper end the availability of sources as well as the low detection efficiency is the limiting factor.

The measurements with two detectors only are reported here, namely, Geli 52 (3.5 cm³ volume) and Geli 123 (13 cm³ volume), because they were the most extensively used. Measurements were made with the smaller detector up to 2.7 MeV and with the larger detector from 2.6 to 4.8 MeV. The V-I characteristic of Geli 52 is given in Fig. 3. The leakage current of Geli 123 was typically a few hundred pA, but exhibited unexplained long-term variations. However, all measurements were done with leakage currents below 4 nA. Other detectors, which in a few instances produced even smaller linewidths, gave consistent results. The time per run was a few minutes at low energies and up to 1 h at high energies. For the fit of Gaussians, data on the lines well into the background were taken. Usually the fit was not good in the tails of the lines. To test whether the discrepancy in these tails produces erroneous parameters, a fit was made down to only 10% of the peak height. The parameters were the same within the uncertainties. The results of some runs

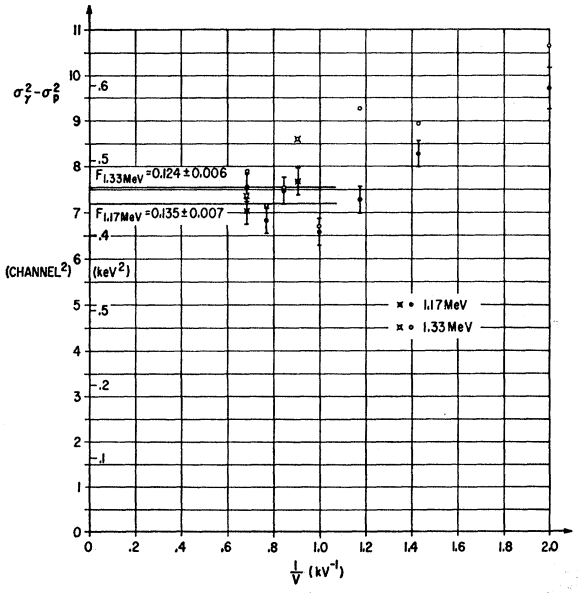

FIG. 19. Net squared rms linewidth $(\sigma_\gamma^2-\sigma_p^2)$ versus the reciprocal detector voltage. The detector thickness is 14 mm. To calculate F and the error, all runs at and above 1 kV were averaged.

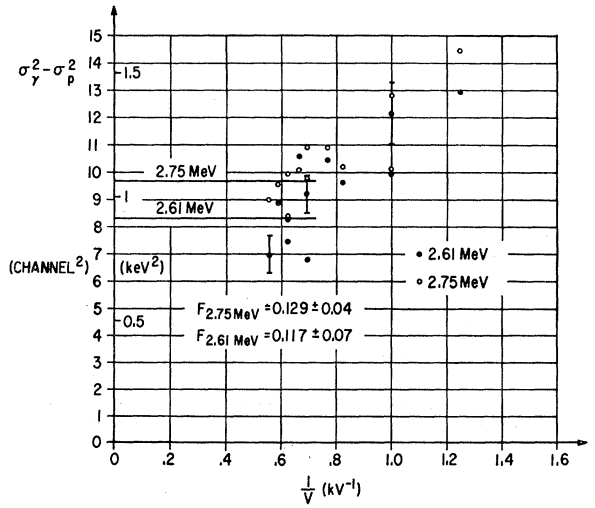

FIG. 20. Net squared linewidths $(\sigma_\gamma^2-\sigma_p^2)$ versus the reciprocal detector voltage. The detector thickness is 14 mm. F and its error are taken from the average of the 7 runs (each about 1 h) above 1.3 kV. The energy spread is 331.2 eV/channel.

[36] H. R. Bilger and I. S. Sherman, Phys. Letters **20**, 513 (1966).

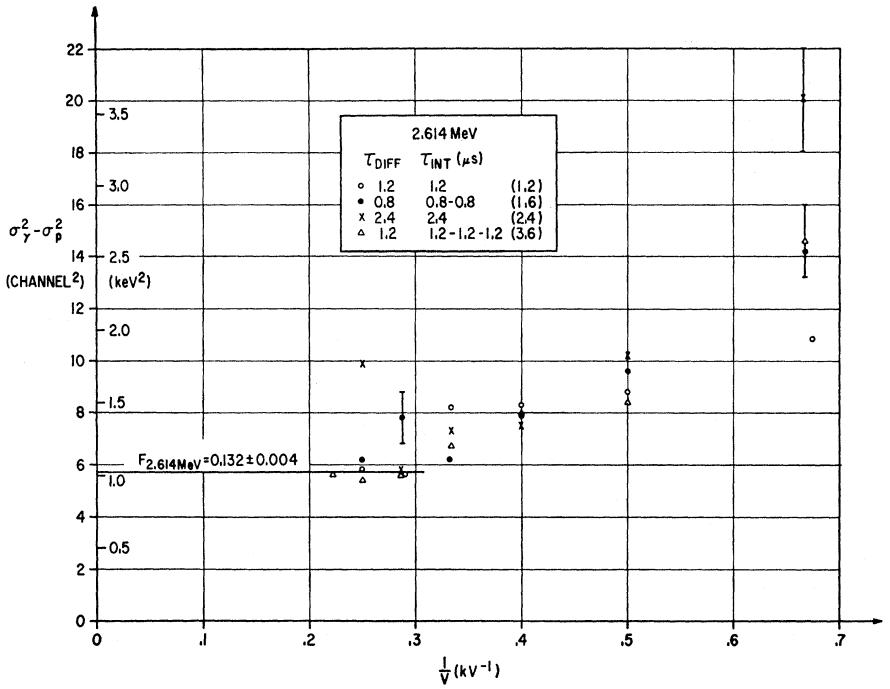

FIG. 21. Net squared rms linewidth ($\sigma_\gamma^2-\sigma_p^2$) versus the reciprocal detector voltage. F is calculated from the measurements above 3000 V, whereby the two points at 8 channels^2 and at 10 channels^2 have been eliminated.

and the fits at various energies are plotted in Figs. 4–10. The parameters were then corrected, if necessary, for the existing nonlinearity and for systematic errors due to the staircase pattern (see Appendix). The parameters thus obtained (with their errors) were then used as the raw data for the subsequent evaluation.

A plot of the location differences between γ line and pulser line versus the reciprocal detector voltage for the various energies is given in Figs. 11–16. A straight line fits the data reasonably well, as is suggested by Eq. 8. (The average electric field strength is given by the quotient of voltage and the active thickness of the detector.) According to Eq. 8, we interpret the intersection of the straight line with the vertical axis as the channel difference for no loss of pairs ($\Delta N=0$) and refer to it as to the zero of the vertical "loss" axis. The rms deviation of the data from the straight line is given in Table II. It is 7.5 eV, or about 2.5 pairs, at 122 keV, and goes up to about 150 eV, or 50 pairs, at 4.8 MeV. These numbers reflect the accuracy and reproducibility of the line locations. In Table II, the *Schubweg* $\mu\tau e=d(N_0/\Delta N)$ at the highest detector voltage used (V_{max}) is given, together with the number of lost pairs, ΔN, at V_{max}. Equations (10) provide an estimate of the expected line broadening due to the loss of pairs during the collection process. It turns out that in all measurements reported here, there should be a negligible contribution[37] to ($\sigma_\gamma^2-\sigma_p^2$) if plotted versus $1/e$ or $1/V$. There is, however, some broadening of the net squared width apparent toward low voltages. This effect becomes more pronounced towards high energies. The broadening stems from tailing on the low-energy side of the γ lines at low voltages, which is due to inefficient collection of a fraction of the events in the line (excessive losses or ballistic deficit). From these considerations, the Fano factor is obtained by inserting into Eq. (3a) the weighted average of the net squared line widths in the limit of high detector voltages. These averages are indicated in Figs. 17–21. As can be seen in Figs. 14–16, 21, runs at different time constants give rise to slightly different losses of pairs. However, only the measurements at 0.6 μsec resulted in an appreciable increase in ($\sigma_\gamma^2-\sigma_p^2$). These measurements were excluded from the averaging. At the gallium energies (3.27–4.80 MeV), measurements at 3.5 and 4.5 kV and at time constants above 0.6 μsec were used to determine F. It may be noted here that the observed unusual broadening of the 3.78- and 4.29-MeV lines indicated an energy separation of the two γ rays which constitute each line that is of the order of 1 keV rather than the 0.1 keV given by Freedman *et al.*[38,39] Therefore, we excluded these two lines from the determinations of F. Tables III and IV collect information pertinent to the evalua-

[37] In the measurements, the quadratic difference $\sigma_\gamma^2-\sigma_p^2$ is taken in each individual run to avoid systematic errors due to pulser linewidth fluctuations. Failure to take this into consideration, besides tailing, might be partly responsible for the erroneous determination of F in Ref. 1.

[38] M. S. Freedman, F. T. Porter, and F. Wagner, Phys. Rev. 151, 899 (1966).

[39] Reference 38 states an energy difference of 0.1±1.5 keV, whereas D.C. Camp [University of California Radiation Laboratory Report No. UCRL 50156] gives 2.0±1.0 keV. It may be noted here that careful measurements and curve fitting will reduce the errors of doublet energies to the order of 0.2 keV or less in the MeV range.

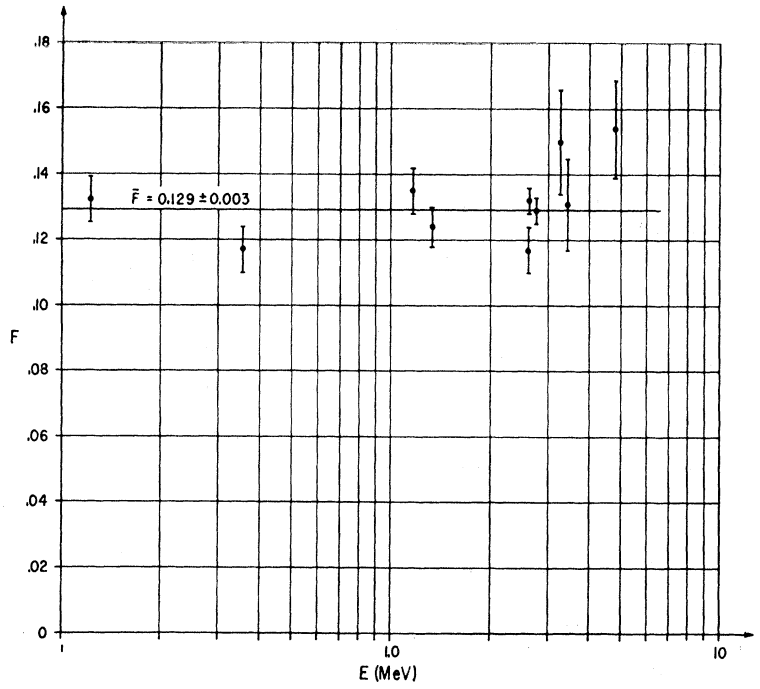

FIG. 22. Results of the Fano-factor measurements given in this paper versus energy. The errors at each point are rms deviations as obtained from averaging the limiting net squared linewidths at a given energy. $\bar{F}$ is the weighted average. The error represents the statistical error of the determinations of the limiting net squared linewidths.

tion of line shifts and linewidths, and they give F as obtained at the various γ energies.

DISCUSSION

The measurements of the width and the location of the lines as a function of the applied detector-field strength proved to be a valuable tool in eliminating systematic errors in F.

Line Shift

At all energies used between 0.122 and 4.80 MeV the line shifts could be represented by straight lines, if plotted versus $1/e$. Under the assumption that the losses are due to recombination, the product $\mu\tau_{\text{eff}}$ in the 4th column in Table III is calculated according to Eq. (9). Using $\mu=4\times10^4$ cm^2/V sec,[40] we obtain τ_{eff} of the order of 25 μsec. This value seems to be somewhat on the low side, since the preparation of the detectors usually starts with material having a lifetime of several hundred μsec. However, it should be remembered that τ_{eff} includes all field-dependent losses. The line shift plots do not reveal, of course, any losses which are not field-dependent. Consequently, any fluctuations due to such losses would add to the fluctuations already considered, and the apparent F would be too large. Plasma losses[7] may serve as a mechanism of field-independent losses, but the ionization densities of fast electrons and holes are smaller than those of heavier and/or slower particles.

In the detector Geli 123, average field strengths are applied which saturate the velocities of both carrier types. In such a case one would expect a saturation of the losses (slope zero at high fields). This could not be detected. The paucity of runs may be responsible for this failure, as well as the fact that the field strengths e given are averages over the whole detector volume, the actual distribution of e depending on the distribution of the residual impurities according to the Poisson equation. Now if recombination occurs, it is likely to occur in the regions of low field strengths, and this may have a considerable smoothing effect on the observed line shift.

Linewidth and Fano Factor

At all energies the net linewidths $\sigma_\gamma^2-\sigma_p^2$ are field-independent above a certain field strength, the value of which depends on the individual detector. At these field strengths the pulser linewidth may already exhibit some broadening due to increased leakage current. Thus the minimum pulser width or even the minimum

TABLE IV. Determinations of F

Energy (MeV)	F
0.122	0.132±0.007
0.356	0.117±0.007
1.17	0.135±0.007
1.33	0.124±0.006
2.61	0.117±0.007
	0.132±0.004
2.75	0.129±0.004
3.27	0.150±0.016
3.44	0.131±0.014
4.80	0.154±0.015

[40] E. G. S. Paige, *Progr. Semicond.* **8**, 1 (1964).

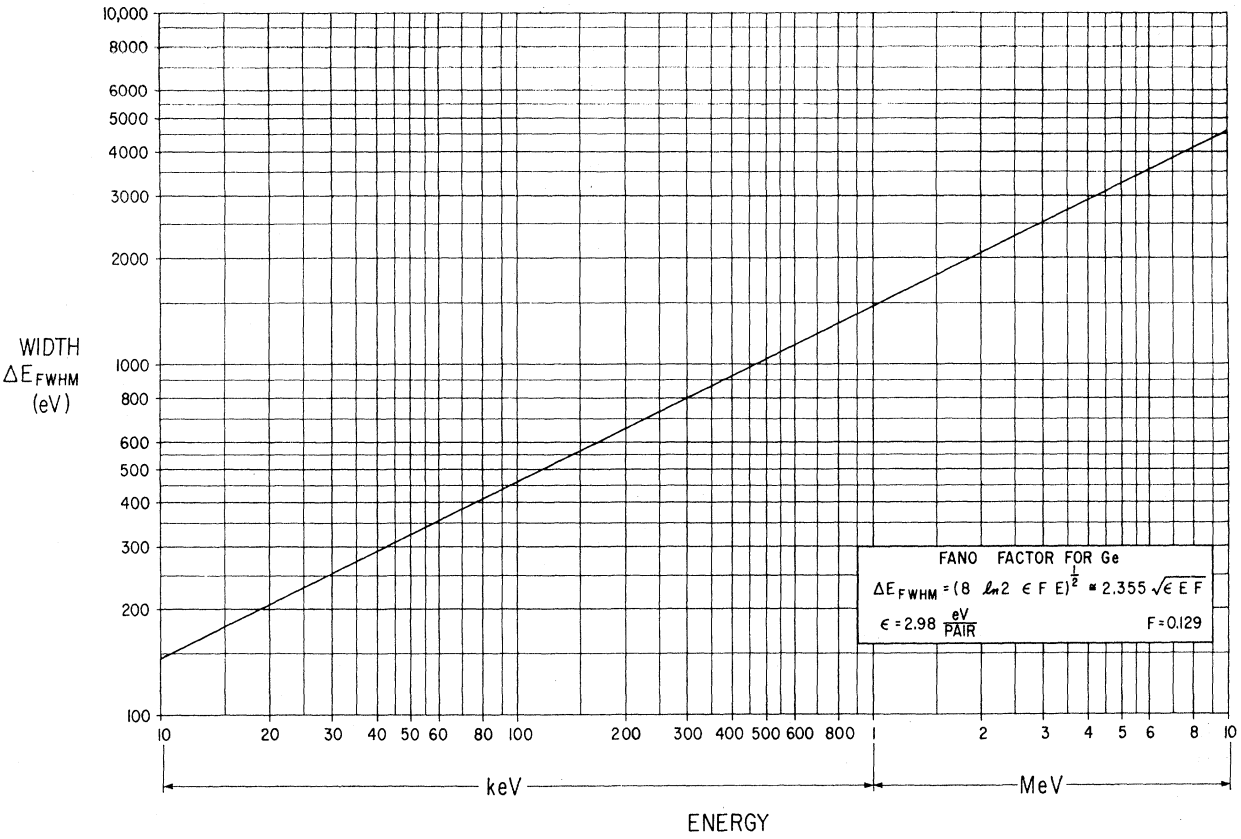

FIG. 23. Graph showing the detector contribution to the FWHM as a function of energy.

γ width versus e are not sufficient data to determine the true Fano factor F.

The line-shift graphs provide quantitative information on possible line broadening due to recombination or ballistic deficit. The number of lost pairs has been found to be too small, at all high field intensities and energies considered, to give rise to an appreciable broadening if the loss process is assumed to be a Poissonian (Gaussian) process. However, it is an experimental fact that $\sigma_\gamma^2-\sigma_p^2$ increases toward low voltages. In those cases, tails on the γ lines towards smaller pulse heights (energies) are observed (with no tailing on the pulser lines). Therefore we conclude that losses occur predominantly in certain regions of the crystal, where the field is less than average owing to uncompensated impurities.

Because of these considerations, we calculate the Fano factor from the average net squared widths $\sigma_\gamma^2-\sigma_p^2$ above a certain field strength, the choice of which depends on γ energy and detector. Table IV summarizes the results from this paper. The Fano factors of Table IV are plotted in Fig. 22. There is no energy dependence apparent. Therefore, we take the weighted average as the best estimate of the Fano factor:

$$\bar{F}=0.129\pm0.003.$$

This result is in agreement with values reported earlier.[10,11,20,41] No difference in linewidth between double-escape and full-energy lines has been observed.

Figure 23 gives the FWHM of γ lines due to F alone as a function of energy.

COMPARISON WITH THEORY

Independence of Energy

F appears to be energy-independent. This aspect can be understood if one realizes that the largest number of pairs is produced in the last generations of the ionization process. These ideas are implicit in Ref. 6 and explicitly worked out in Ref. 5. One significant step further in Fano-factor measurements would be to show whether or not F differs above and below the K absorption edge, which is at 11 keV. The result will give information whether F is influenced by the fact that transitions from and into the K shell are involved. At the moment one would expect that no change in F occurs. F measurements at 10 keV are now possible. The net linewidth will be of the order of 150 eV (see Fig. 25).

[41] See E. Baldinger and G. Matile, Helv. Phys. Acta **39**, 573 (1966).

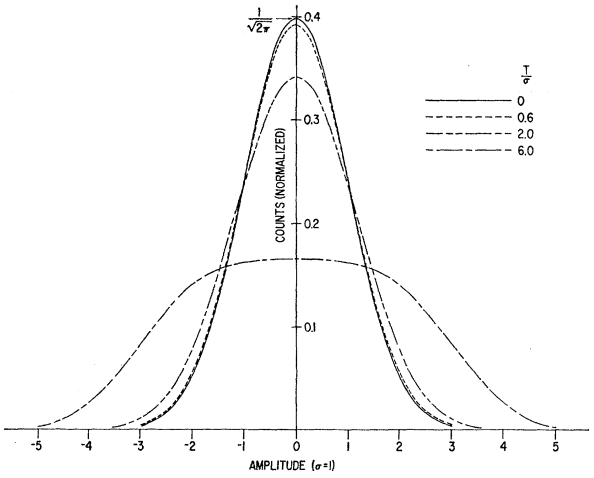

FIG. 24. Convoluted curves consisting of a Gaussian with $\sigma=1$ and constant drift (rectanglular curve) of variable width T. The shape of the curve with $T=2\sigma$ is still close to Gaussian.

About the Value

The most striking feature of F besides its energy independence is its small value. As the investigations in Ref. 1 show, $F=0.32$ would have been compatible with Shockley's model for ϵ and Roosbroeck's interpretation of F. Since the actual F is 2.3 times smaller, we are forced to modify or reinterpret either Roosbroeck's interpretation or Shockley's model itself.[11,22] It is interesting to note, however, that Roosbroeck's approach provides $F\approx 0.12$ for the limiting case of no production of phonons. This would eliminate the awkward problem of explaining the creation of 47 phonons per ionization event,[1] but it leaves the problem of understanding the then large value of ϵ. A closer examination of the energy-level approach (see section on theory) provides a way out. As can be seen in that section, the level approach can explain $0\leq F\leq\frac{1}{3}$ (without phonon losses) by adjusting the distribution of levels or the respective transition probabilities.

If we use Eqs. (6) and (7) with $F=0.129$, $\epsilon=2.98$ eV, and an optical energy gap of germanium of about 0.9 eV, we get a "conduction band" of width 3.7 eV and a "valence band" of 0.5 eV. The validity of this picture depends, of course, on results on the band configuration from independent experiments.

Translating this model into Roosbroeck's approach, one has to increase the size of the energy unit, or in other words, introduce a threshold energy E_i which is much larger than E_g. Let us assume that no phonons are produced in Roosbroeck's sense. The limiting relative yield Y is then

$$Y \text{ (no phonons)} = \tfrac{2}{3} = E_i/\epsilon \quad \text{or} \quad E_i = \tfrac{2}{3}\epsilon \simeq 2 \text{ eV} > E_g.$$

This estimate tells us that the dominating transitions involve gaps of the order of 2 eV.

ACKNOWLEDGMENTS

The author is grateful for the interest and assistance of a number of people, among them H. M. Mann for stimulating discussions; H. W. Helenberg for his persistent and successful attempts to get high-resolution detectors into operation; J. D. Simpson for providing his curve-fitting program and J. P. Marion for modifications on it; M. S. Freedman and M. C. Oselka for help in preparing the sources; H. H. Bolotin for lending some of his apparatus and helping in measurements; and the people involved in the design and construction of detector systems and electronics: R. G. Roddick, S. J. Rudnick, J. G. Semmelman, M. G. Strauss, and in particular I. S. Sherman.

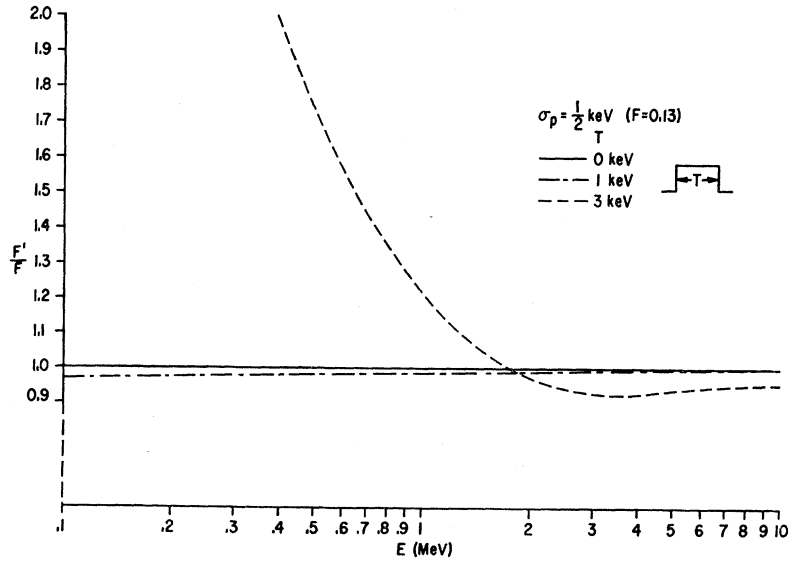

FIG. 25. Apparent Fano factor F' versus energy, if constant drift is present. F' is obtained by as imulated evaluation of the Fano factor, wherein the convoluted curves of the type shown in Fig. 24 were processed like a regular run (see text). $F=0.13$ and $\sigma_p=0.5$ keV were used for the calculations. The F'/F for $T=2\sigma_p$ nowhere deviates more than 4% from $F'/F=1$ in the given energy range.

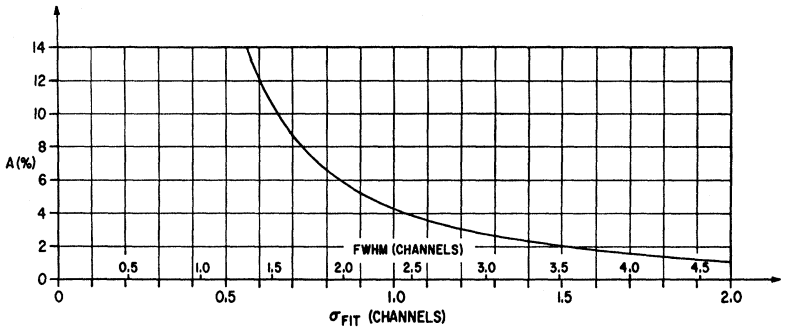

FIG. 26. Staircase correction in percent as a function of the least-squares-fitted width (channels). The correction is less than 1% for FWHM $\geq$ (5 channels).

APPENDIX

Drift

The simple case of rectangular drift (a constant drift speed of the apparatus during the time of measurement) is treated here. A normalized rectangular pattern of variable width T is folded into a Gaussian (Fig. 24). Then a Gaussian plus background is fitted into the resulting convoluted curve. To study the effect of such a drift on the apparent F, we simulated a run with a pulser line of $\sigma_p=0.5$ keV and γ lines with widths

$$\sigma_\gamma^2=\sigma_p^2+\epsilon EF,$$

where $\epsilon=2.98$ eV/pair and $F=0.13$. Various energies are chosen. As an example, we chose $T=1$ keV and $T=3$ keV in comparison with $T=0$ keV (no drift). The resulting least-squares-fitted effective widths are σ_γ' and σ_p'. Then we obtain the apparent Fano factor F' as

$$F'/F=[(\sigma_\gamma')^2-(\sigma_p')^2]/[\sigma_\gamma^2-\sigma_p^2],$$

which is given in Fig. 25 as a function of energy. As can be seen, for $T/2\sigma=1$ the error is less than 5% in the given energy range. For $T/2\sigma=3$, the deviations are pronounced at low energies and tend to increase the apparent Fano factor.

The above considerations hold for rectangular drift. Assume on the other hand, that the drift (or related line-broadening effects which affect both pulser and γ lines) itself can be approximated by a Gaussian. In such a case the widths due to noise, to F, and to drift all add quadratically, and no error is made in F, if the given procedure is applied.

Staircase-Pattern Correction

With decreasing width of a line systematic errors are introduced, because the multichannel pattern is discrete. Rather than to apply Sheppard's correction,[42] we calculated staircase patterns from a true Gaussian for various ratios of σ/(channel width). Two symmetry cases were calculated, one with one peak channel in the center and another with two equally high peak channels on either side of the center. The computer then calculates σ_{fit}, which is larger than the true σ. The deviations were the same for both symmetries. The results are plotted in Fig. 26, which relates the true σ to σ_{fit} by

$$\sigma=\sigma_{\text{fit}}(1-A/100).$$

The curve shows that this type of error becomes smaller than 1% for FWHM> (5 channels). One should therefore tend to spread the FWHM of a line over 5 channels or more, if no opposing conditions exist.

Ballistic Deficit

The calculation is extended to a filter consisting of one differentiating RC and n integrating RC's, all having the same time constant τ. The input pulse is a constant current pulse of duration T. A second-order approximation for the deficit is[23]

$$\Delta N/N_0=-\left\{\frac{\frac{1}{2}[d^2g(t)/dt^2]_{t_0}}{[g(t_0)]}\right\}\int_0^T[\tfrac{1}{2}T-\tau]^2\frac{1}{T}d\tau,$$

where $g(t)$ is the response of the filter to a current δ pulse and t_0 is the time of maximum pulse height. The result is $\Delta N/N_0=(1/24)(T/\tau)^2(1/n)$. For a given T the deficit can be minimized by maximizing $n\tau^2$. Thus, it proves to be a better procedure to filter with one integrating time constant with a large value than with several time constants of proportionally smaller individual τ's.

[42] *Handbook of Chemistry and Physics, 44th edition* (Chemical Rubber Publishing Co., Cleveland, Ohio, 1963), p. 338.